Changes in C-S-H of Alkali-Activated Slag and Cement Pastes After Accelerated Carbonation

F. Puertas, M. Palacios

Eduardo Torroja Institute (CSIC) P. O. Box 19002, 28080 Madrid (Spain)

ABSTRACT

C-S-H gel of waterglass- and NaOH-activated slag pastes (AAS) was analysed after accelerated carbonation and compared to the carbonation of C-S-H in Portland cement pastes. TG/DTA, FTIR and ^{29}Si and ^{27}Al NMR MAS analyses were used to determine the changes in the C-S-H gel.

The different structure and composition of the C-S-H gel in AAS and Portland cement pastes before carbonation is the reason of the different carbonation mechanism in both systems. The carbonation of the C-S-H gel of AAS and Portland conducts to $CaCO_3$, silica gel and a C-S-H gel with a low Ca/Si. However, in AAS pastes, the Al in the silicate chains in the C-S-H gel is removed and a compound with Al tetrahedral is formed, development not observed in Portland cement pastes.

1.- Introduction

Carbonation process affects the durability of concrete due to causes a decline in the aqueous phase pH that leads to depassivation and subsequent corrosion of the reinforcing steel (1). Carbonation of Portland cement has been studied deeply by several authors (2,3). Portland cement mortars under accelerated carbonation suffer a superficial carbonation as a result of the reaction of atmospheric CO_2 with the $Ca(OH)_2$ (4). The $CaCO_3$ precipitated in the pores prevents the passage of CO_2 into deeper layers of the mortar. Other authors (2) have reported that in Portland cement pastes exposed to very severe carbonation conditions, carbonation also takes place in the C-S-H gel, which breaks down into $CaCO_3$ and silica gel.

On the contrary, the carbonation of alkali-activated slag (AAS) systems has received much less attention and the results obtained (5 -7) are quite variable. Previous works (4) concluded that in AAS mortars the carbonation takes place directly in the C-S-H gel (4, 6). Additionally, Bin and Xincheng (7) concluded that the carbonation rate in Portland cement concretes was higher than in the respective AAS concretes due to the hydrated products formed in activated slag cements are less alkaline than Portland cement hydration products and the lower

permeability of AAS concretes that hinders the penetration of water and CO_2.

Several authors have suggested that the behaviour of AAS cement with respect to carbonation depends on the nature of the activator solution used. Deja y Malolepszy[13] concluded that carbonation penetrates less deeply when the alkali activator used is a waterglass solution. Puertas et al (4), in turn, deduced that when waterglass was used, decalcification of the C-S-H gel as a result of carbonation was observed to entail an increase in porosity and a decrease in mechanical strength; whereas when the alkaline activator was NaOH, the mortars became more compact after carbonation, inducing a refinement of the porous structure and an enhancement of mechanical strength.

Therefore, very few is known about the chemical reactions between these alkaline cements and atmospheric CO_2 and about the difference with respect to the carbonation process of Portland cement pastes. In this case, it is not clear if the different composition and structure of the main reaction product, C-S-H gel, originate differences in the carbonation process in AAS pastes with respect to Portland cement pastes. To this end, waterglass- and NaOH-activated slag paste was subjected to accelerated carbonation and the microstructure of the main reaction products formed was analysed using TG/DTA, FTIR and NMR techniques.

2.- Experimental Procedure

2.1.- Materials and pastes preparation

Vitreous slag from a Spanish blast furnace and CEM I 42.5 Portland cement were used. Table 1 gives the chemical composition and specific surface of these materials. AAS and Portland cement pastes were prepared with a liquid/solid ratio of 0.5 and 0.4, respectively. Two different alkaline solutions were employed to activate the slag: a waterglass ($Na_2O{\cdot}nSiO_2{\cdot}mH_2O$ + NaOH) solution with a Na_2O/SiO_2 ratio = 1.0, and a NaOH solution.

Table 1. Chemical composition of blast furnace slag and cement

%	CaO	SiO_2	Al_2O_3	MgO	Fe_2O_3	SO_3	S^{2-}	Na_2O	K_2O	L.O.I.	I.R.
Blast furnace slag	41.37	34.95	13.11	7.12	0.69	0.04	1.92	0.27	0.23	2.02	0.11
Portland cement	64.41	17.91	5.17	1.30	3.85	2.64	-	0.39	0.78	0.78	0.29
Specific surface (Blaine)	Cement: 360 m^2/kg						Slag: 325 m^2/kg				

L.O.I. = loss on ignition I.R.= insoluble residue

2.2.- Carbonation test

The pastes were stored in a humidity chamber (98% RH, 20±2ºC) for 28 days and then ground and placed in a carbonation chamber where the relative humidity was kept at 43.2% in a K_2CO_3 solution (*E 104-02 ASTM. "Maintaining Constant Relative Humidity by Means of Aqueous Solutions"*). The pastes specimens were removed after 4 weeks of exposure. The carbonated pastes were treated as described by Takashima (8) which consists in the selective dissolution of the components in the AAS and Portland cement pastes by a methanol-salicylic solution. The C-S-H gel in pastes, as well as the tricalcium and dicalcium silicates, free lime, calcium hydroxide, ettringite and monosulphoaluminate phase are soluble in the test medium (methanol - salicylic acid).

2.3.- Tests conducted

AAS pastes and the Portland cement pastes were studied before and after carbonation by different techniques:

a) Thermogravimetric-differential analysis (TG/DTA). A Labsys SETARAM facility was used. The samples were heated from 100 ºC to 1050 ºC at a rate of 10 ºC/min in air atmosphere.

b) Fourier transform infrared (FTIR) spectroscopy. An ATIMATTSON, Genesis FTIR-TM spectrometer was used. KBr pellets (1.0 mg of sample to 300 mg of KBr) were prepared.

c) ^{29}Si and ^{27}Al magic angle solid nuclear magnetic resonance (MAS NMR). A BRUKER MSL 400 spectrometer was used. The ^{29}Si and ^{27}Al spectra were obtained at resonance frequencies of 79.49 and 104.2 MHz, respectively.

3.- Results

3.1.- Thermogravimetric-differential analysis (TG/DTA)

Table 2 shows the weight loss of pastes in two temperature ranges, 100ºC – 600ºC and 600ºC – 1050ºC. Weight loss between 100ºC and 600ºC was associated with reaction product dehydration. In the Portland cement pastes, the C-S-H gel, ettringite, monosulphoaluminate and portlandite dehydrated in that range, whereas in the waterglass or NaOH-AAS pastes, only the C-S-H gel dehydrated. Table 2 shows that weight loss was similar, on the order of 9%, for the non-carbonated waterglass-AAS paste and the likewise non-carbonated Portland cement paste. However, the weight loss of NaOH-AAS pastes non-carbonated was lower (~ 7.60%). Carbonation had practically no effect on the weight loss in waterglass-AAS and

Portland cement pastes in this temperature range. However, the weight loss of NaOH-AAS pastes was 2% greater in the carbonated than the non-carbonated paste.

Weight loss in the different pastes at temperatures of from 600ºC to 1050ºC was due essentially to decarbonation. In pastes not subjected to accelerated carbonation, such weight loss was due to weathering and was much more intense in Portland cement than in the other two types of pastes. The weight loss was greater in NaOH-activated than in waterglass-AAS pastes. After exposure to accelerated carbonation, the greatest weight loss in this range of temperature was recorded for Portland cement pastes (18.73%), followed in this case by waterglass-AAS pastes, where the weight loss was slightly higher than in pastes made with NaOH-AAS.

Table 2.- Paste weight loss before and after carbonation

PASTE	WEIGHT LOSS (%)			
	100ºC – 600ºC		600ºC – 1050ºC	
	NON-CARBONATED	CARBONATED	NON-CARBONATED	CARBONATED
Portland cement	9.51 %	9.76 %	9.41 %	18.73 %
Waterglass-AAS	9.15 %	9.00 %	1.18 %	7.39 %
NaOH-AAS	7.60 %	9.00 %	3.30 %	6.34 %

3.2.- Fourier transform infrared spectroscopy

Figure 1 shows the infrared spectra for the AAS and Portland cement pastes before and after accelerated carbonation. The infrared spectra for the carbonated pastes treated with the Takashima method are also presented in this Figure.

The infrared spectrum for Portland cement pastes at 28 days of curing (Figure 1a) indicates the presence of calcite (1429 cm^{-1}, 875 cm^{-1} and 710 cm^{-1}) as a result of the weathering. After four weeks of carbonation, the vibration band associated to the portlandite at 3642 cm^{-1} (O -H bond) had disappeared while the initial calcite was still present and aragonite is formed (1483 cm^{-1}, 1452 cm^{-1}, 875 cm^{-1}, 854 cm^{-1}, 713 cm^{-1}). A shifted to higher wavenumbers of the Si-O bonds in the silicate chains is observed, which inidicates and enrichment in Si of the C-S-H gel. An increment of the intensitity of the vibration band at around 1200 cm^{-1} – 1000 cm^{-1} is observed after the Takashima test (8). That wavenumber interval contains both the vibrations associated with the silica gel Si-O bond (1150 cm^{-1}, 1070 cm^{-1}, 950 cm^{-1}, 800 cm^{-1} and 470cm^{-1}) and the Al-O bond vibrations which, together with the increased intensity of the bands appearing at 790 cm^{-1}, 667 cm^{-1}, 600 cm^{-1} and 456 cm^{-1}, may be indicative of the formation of alumina (9).

Calcite was detected in the AAS pastes at 28 days of curing due to they were partially weathered. Aragonite appeared as carbonation progressed. In addition, the shift in the bands for the Si-O bonds to larger wavenumbers was interpreted to mean a higher Si content in the C-S-H gel. The spectra for the carbonated samples subjected to the Takashima procedure exhibited a very wide band between 1000 cm^{-1} and 1200 cm^{-1}, which may include overlapping vibration bands corresponding to the silica gel (10) and possibly alumina or other aluminium compound with tetrahedral coordination.

3.3.- ^{29}Si and ^{27}Al MAS NMR

Figure 2 depicts the ^{29}Si MAS NMR spectra for the cement and slag pastes before and after carbonation. Tables 2 and 3 show the data obtained after deconvoluting those spectra.

The signal at -72 ppm on the ^{29}Si MAS NMR spectrum for non-carbonated Portland cement paste was assignabel to Q^0 Si units in C_3S and C_2S of clinker. The signals observed at -79.4 and -84.7 ppm were attributed, respectively, to Q^1 and Q^2 Si units in the C-S-H gel (11). The ^{29}Si MAS NMR spectrum for the waterglass- and NaOH-AAS pastes cured for 28 days had two signals, at around -69.0 ppm and -74.0 ppm, attributed to the Q^0 and Q^1 Si units in the anhydrous slag. In addition, the ^{29}Si MAS NMR spectrum for the waterglass-AAS pastes contained five signals around – 78.5 ppm, -82.0 ppm, -85.5ppm, -89.6 ppm y –94.1 ppm, attributed to Q^1, Q^2(1Al), Q^2(1Al), Q^2, Q^3(1Al) and Q^3 Si units, respectively (11).

After four weeks of carbonation, the ^{29}Si MAS NMR spectra for the Portland cement pastes still showed signals at -72 ppm, -79.5 ppm and -85.3 ppm, but other new peaks appeared at -92.7 ppm, -98.3 ppm, -103.6 ppm and -109 ppm, attributable to Q^2(2H), Q^3, Q^3(1H) and Q^4 Si units, respectively (2,12). Carbonation of AAS pastes produces the disappearance of the signals characteristic of Q^2(1Al) and Q^3(1Al) Si units (around -82 ppm and -89.5 ppm, respectively). Moreover, three signals appeared at –92.0 ppm, -102.7 ppm and -109.0 ppm, attributed to Q^2(2H), Q^3(1H) and Q^4 units, respectively. The ^{27}Al MAS NMR spectrum for Portland cement paste contained several signals (see Table 4): at 66 ppm, associated to the tetrahedral Al in the anhydrous calcium aluminate; at 12.7 ppm, attributed to the octahedral Al in the ettringite; at 7.9 ppm, attributed to monosulphonate, and at 2.44 ppm, corresponding to the octahedral Al in the hydrated aluminium phases (1,11). After four weeks of carbonation, the percentage of Al associated to ettringite and the octahedral Al in the hydrated aluminate phases was observed to decline, while the percentage of tetrahedral Al units increased. The spectra for the AAS pastes had three signals: ~61.0 ppm, ~33.0 ppm and ~8.0 ppm, corresponding to tetrahedral, pentahedral and octahedral Al units, respectively. In all cases,

carbonation induced a decline in the octahedral Al content and a rise in the percentage of tetrahedral Al.

^{29}Si and ^{27}Al NMR spectra of carbonated waterglass-AAS paste after Takashima procedure is showed in Figure 4. The signals corresponding to anhydrous slag (-61.0 ppm and –73.5 ppm) on the ^{29}Si NMR spectra were observed to intensify. At the same time, signals corresponding to the Q^2 and Q^3 Si units are observed at –85 ppm and –95 ppmm, respectively. The ^{27}Al NMR spectra for these same samples confirmed that the majority of tetrahedrical Al units (≈86%).

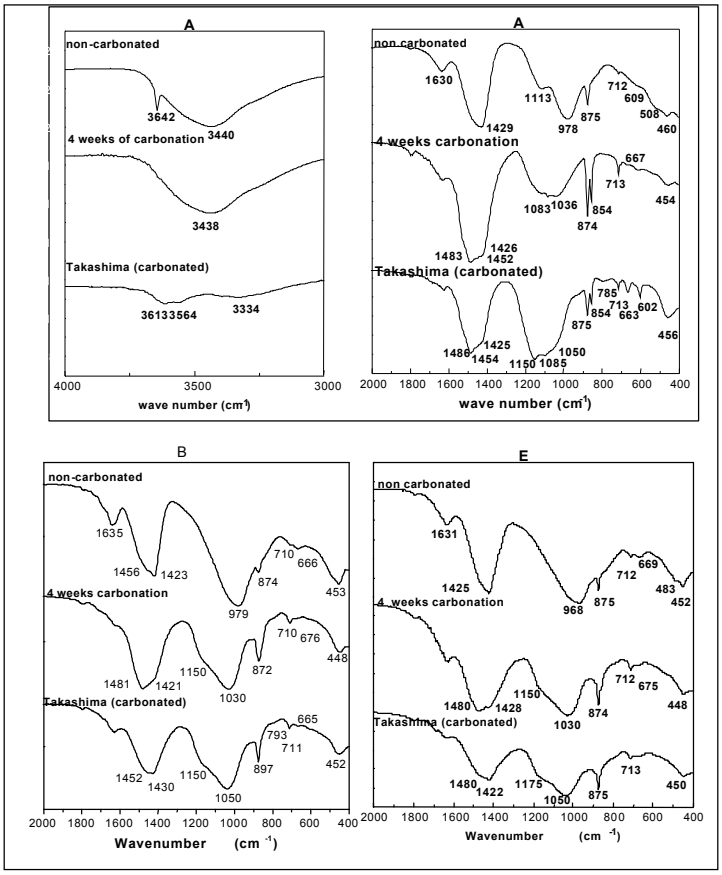

Fig. 1.- FTIR spectra for cement and AAS pastes: 28 days after curing, before and after carbonation and after Takashima treatment

4.- Discussion

The different structure and composition of the C-S-H gel in AAS and Portland cement pastes before carbonation is the re ason of the different carbonation mechanism in both systems. However, according to the FTIR and MAS NMR results, Portland cement and AAS paste carbonation generates $CaCO_3$, C-S-H gel with a low Ca content, silica gel and possibly alumina.

Table 2.- Deconvolution of pastes cured for 28 days

PASTES	Q^0	Q^1 (anhydrous)	Q^1	Q^2(1Al)	Q^2	Q^3 (1Al)	Q^2 (2H)
Portland cement	-72.2ppm W=4.90 I=32.58%		-79.4ppm 4.90 43.44 %		-84.7ppm 4.90 23.98 %		
Waterglass-AAS	-69.0ppm W = 7.20 I = 4.75%	-74.9ppm 7.20 22.86 %	-78.8ppm 3.79 9.73 %	-82.0ppm 3.79 19.31%	-85.6ppm 3.79 26.11%	-89.6ppm 3.79 10.56 %	-94.1ppm 3.79 6.67 %
NaOH-AAS	-69.0ppm W=5.50 I=7.94 %	-74.2ppm 5.50 23.81 %	-78.5ppm 4.20 17.58 %	-82.0ppm 4.20 23.64 %	-85.5ppm 4.20 16.56 %	-89.8ppm 4.20 6.54 %	-94.9ppm 4.20 3.94 %

Table 3.- Deconvolution of pastes after 4 weeks of carbonation

Pasta	Q^0	Q^1 (Anhidro)	Q^1 (Final cadena)	Q^2	Q^2 (2H)	Q^3	Q^3(1H)	Q^4
Portland cement	-71.7ppm W=5.61 I=14.71%		-79.5ppm 5.61 22.66 %	-85.3ppm 5.51 22.15 %	-92.7ppm 5.51 11.04 %	-98.3ppm 5.51 13.32 %	-103.6ppm 5.51 9.11 %	-109.0ppm 5.51 7.02 %
Waterglass-AAS	-69.5ppm W = 5.30 I = 4.68%	-74.2ppm 5.30 8.73%	-78.9ppm 6.70 16.16 %	-86.0ppm 6.80 13.60 %	-92.0ppm 6.80 15.21 %	-96.9ppm 6.80 18.01 %	-102.7ppm 6.80 17.21 %	-109.0ppm 6.80 6.40 %
NaOH-AAS	-69.0ppm W=6.3 6.07 %	-74.3 ppm 6.30 17.80 %	-79.7ppm 7.0 17.08 %	-86.5ppm 7.0 14.38 %	-92.0ppm 7.0 13.48 %	-97.3ppm 7.0 17.08 %	-103.1ppm 7.0 10.53 %	-109.0ppm 7.0 3.60 %

Table 4.- Deconvolution of ^{27}Al MAS NMR for pastes before and after 4 weeks of carbonation

	Cured for 28 days			4 weeks of carbonation		
PASTES	Al_t	Al_p	Al_o	Al_t	Al_p	Al_o
Portland cement	65.9 ppm W = 23.75 I = 29.38%		12.7 ppm 4.68 40.47 % 7.9 ppm 4.68 17.34 % 2.4 ppm 4.68 12.81 %	54.8 ppm 11.92 53.46 %		12.9 ppm 3.41 34.54 % 8.7 ppm 3.41 7.10 % 3.5 ppm 3.41 4.90 %
Waterglass-AAS	59.0 ppm W = 19.09 I = 79.06 %	32.1ppm 17.21 5.77 %	8.2 ppm 10.20 15.17 %	55.6 ppm 13.11 88.11 %	39.3 ppm 11.82 6.90 %	8.5 ppm 7.01 4.99 %
NaOH-AAS	61.1 ppm 21.16 77.30 %	31.8ppm 19.08 6.64 %	8.6 ppm 11.31 16.06 %	55.7 ppm 13.21 85.04 %	38.0 ppm 11.91 8.42 %	8.9 ppm 7.06 6.54%

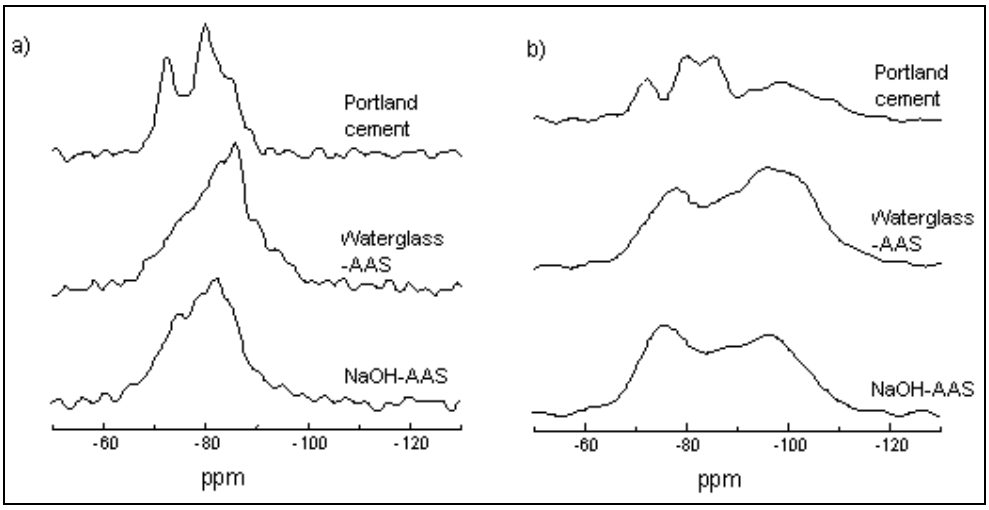

Fig. 2.- ^{29}Si MAS NMR spectra for pastes: a) cured for 28 days; b) after 4 weeks of carbonation

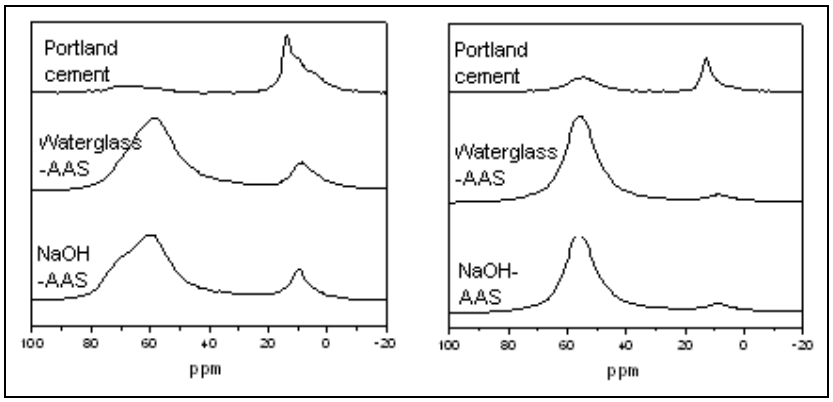

Fig. 3.- ^{29}Al RMN spectra of pastes: a) cured for 28 days; b) after 4 weeks of carbonation

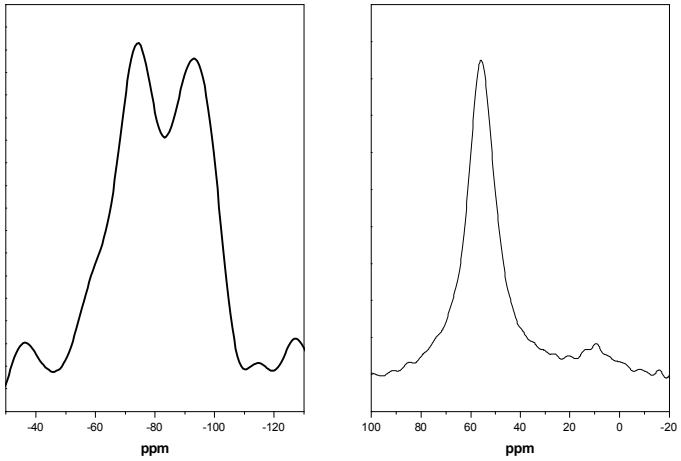

Fig. 4.- ^{29}Si and ^{27}Al NMR of waterglas-activated slag pastes after 4 weeks of carbonation and MeOH-salicylic acid treatment

The TG/TDA results (Table 2) indicate that carbonate precipitation alter carbonation test is much more intense in Portland cement than in AAS pastes, since the loss of weight in the 600ºC-1050ºC, associated with the decomposition of $CaCO_3$, is greater in Portland cement. The explanation for this finding should be sought in the greater amounts of Ca susceptible to interaction with the CO2 dissolved in the aqueous phase in Portland cement pastes where carbonation takes place both in the portlandite and in the C-S-H gel. In AAS, in turn, carbonation occurs directly in the C-S-H gel (4,6).

According to the literature (1, 13) in Portland cement pastes atmospheric CO_2 dissolved in aqueous phase reacts very quickly with portlandite to form $CaCO_3$ (eq. [1]). In very severe carbonation processes, the reaction progresses and the CO_2(s) also react with the C-S-H gel, forming $CaCO_3$ and silica gel (eq. [2]) (2).

$$Ca(OH)_2 + CO_2(s) \rightarrow CaCO_3 + 2\ H_2O \quad \text{eq. [1]}$$

$$x\ CaO{\cdot}SiO_2 \cdot y\ H_2O + CO_2(s) \Leftrightarrow SiO_2{\cdot}y\ H_2O + x\ CaCO_3 + H_2O \quad \text{eq. [2]}$$

The results obtained with FTIR and MAS NMR confirm these reactions. The infrared spectra in Figure 1a shows that after 4 weeks of carbonation the portlandite (3642 cm^{-1}) disappears and $CaCO_3$ in form of calcite and aragonite are formed (eq. [1]). In addition, the bands characteristic of the Si-O bonds shift to higher wavenumbers due to the enrichment in Si of the C-S-H gel. This enrichment originates silica gel (eq. [2]). These results agree with the ^{29}Si MAS NMR results that indicate that after four weeks of carbonation a higher condensation in the CSH gel is observed and, in addition to the Q^1 and Q^2 Si units characteristic of the CSH gel (-79.5 ppm, -84.7 ppm), a third signal associated with Q^3 Si units appears at -98.3 ppm. Three other signals characteristic of silica gel also develop, at -92.7 ppm, -103.6 ppm and -109.0 ppm, respectively attributed to Q^2(2H), Q^3(1H) and Q^4 Si units. The ^{27}Al MAS NMR spectrum for the carbonated cement paste, and the spectrum for the carbonated paste treated later to Takashima procedure, shows a rise in the percentage of tetrahedral Al units. This finding, along with the increase in the Al-O bond vibration bands observed in FTIR, may be indicative of the formation of alumina, possibly γ-$Al(OH)_3$ (≈ 1030 cm^{-1}, 980 cm^{-1}, 790 cm^{-1}, 667 cm^{-1}, 600 cm^{-1} and 456 cm^{-1}), in which Al is mainly tetrahedrally coordinated. According to Vázquez (10) , this alumina forms as a result of the carbonation and breakdown of the ettringite and monosulphoaluminate phases of hydrated cement pastes.

In AAS pastes, on the contrary, carbonation takes place directly in the C-S-H gel (4, 6). The C-S-H gel in AAS pastes has a dreierketten structure as in Portland cement. However, compared to Portland cement paste C-S-H gel, the C-S-H gel in alkali-activated slag pastes is made up of longer chains (n≈8.0) with a lower Ca/Si ratio (≈0.6-1.0) with Al partially replacing Si (14, 16). The nature of the alkaline activator generates structural differences in AAS C-S-H gel. According

to the results of ^{29}Si MAS NMR at 28 days of curing, waterglass-AAS C-S-H gel has a low Ca/Si ratio (0.6-0.7) (16) and consequently in the dreierketten structure not all the non-bridge silicate tetrahedra bond to the central Ca-O layer: some, rather, are protonated. Since the C-S-H gel in NaOH-AAS pastes, on the contrary, has a higher Ca/Si ratio, on the order of 0.9-1.0 (16), all the silicate tetrahedra with the exception of the bridge silicates are bonded to the Ca-O layer.

The carbonation of the waterglass- and NaOH-AAS paste is produced directly on the C-S-H gel (see Fig. 5). The CO_2 dissolved in the aqueous phase reacts with the Ca^{2+} ions located in the interlayer zone, between the silicate chains of the C-S-H gel, as the oxygen atoms formerly bonded to Ca^{2+} ions become protonated. The low relative humidity (RH=43%) at which carbonation was conducted favours the partial elimination of water molecules coordinated with the OH of the silanol groups, and the formation of bonds between the Si units on the different silicate chains. Consequently, the ^{29}Si MAS NMR spectra show the signals characteristics of C-S-H gel and three new signals characteristic of silica gel at -92 ppm, 103 ppm and -107 ppm attributed to the $Q^2(2H)$, $Q^3(H)$ and Q^4 Si units, respectively.

The enrichment in Si of the waterglass- and NaOH-AAS C-S-H after carbonation is deduced from the shift to higher wavenumbers of the Si-O bonds observed by FTIR. In pastes treated with the Takashima method, the band in the vicinity of 1200 cm^{-1} – 1000 cm^{-1} was observed to widen. This is the interval where the Si-O and Al-O vibration bands characteristic of the silica gel and an aluminium compound with tetrahedral coordination overlap. The formation of this aluminium compound explains the heightened intensity of the tetrahedral Al signal on the ^{27}Al MAS NMR spectra of carbonated waterglass-AAS pastes. Unlike the mechanism described for Portland cement pastes, in AAS pastes, the aluminium compound with tetrahedral coordination is formed from the Al in the silicate chains in the C-S-H gel, as inferred by the disappearance of the $Q^2(1Al)$ and $Q^3(1Al)$ Si units from the ^{29}Si MAS NMR spectra.

C-S-H gel in alkali-activated slag pastes is less basic (lower Ca/Si ratio) than the C-S-H gel of Portland cement pastes, for that the C-S-H of alkali-activated slag pastes could be lesser vulnerable to suffer carbonation than C-S-H of Portland cement pastes. However, in the severe carbonation conditions in which the pastes have been tested both C-S-H gels suffer carbonation in similar proportion. Previous results (4) concluded that alkali-activated slag mortars are more sensible to carbonation than Portland cement mortars. The reason of this different behaviour is that in the alkali-activated slag mortars the carbonation is produced directly on the C-S-H gel, however in Portland cement pastes, the carbonation takes place first on the portlandite and subsequently on the C-S-H gel.

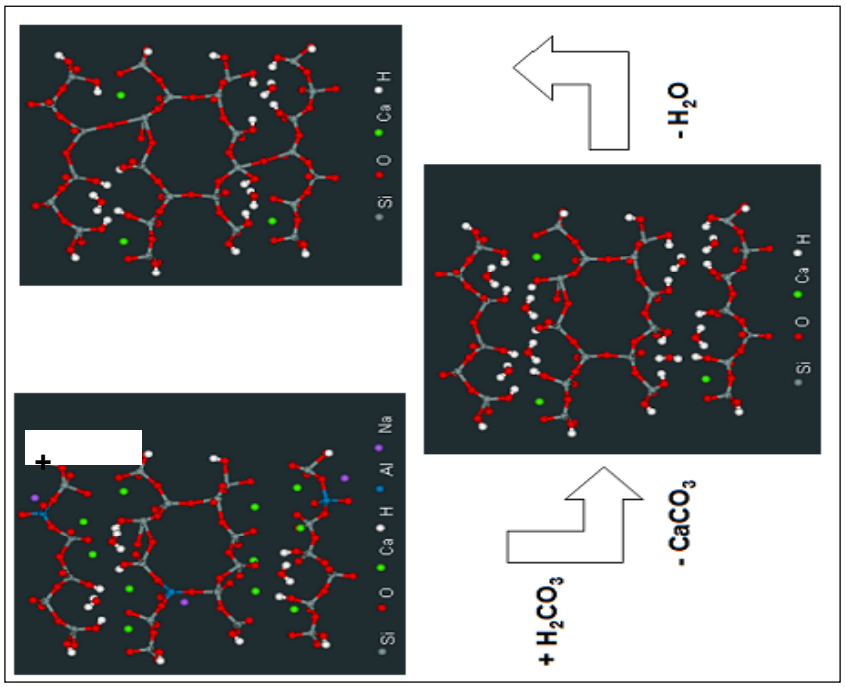

Fig. 5.- Scheme of carbonation of alkali-activated slag pastes

5.- Conclusions

The carbonation mechanism is not the same in the Portland and AAS systems.

1.- In Portland cement pastes, atmospheric CO_2 dissolves in the aqueous phase water reacts very quickly with portlandite to form $CaCO_3$. In very severe carbonation processes, the reaction progresses and the CO_2 also reacts with the C-S-H gel, forming $CaCO_3$ and silica gel. In addition, during carbonation the ettringite and monosulphoaluminate phases break down to form alumina.

2.- The carbonation mechanism in the waterglass - and NaOH-AAS paste C-S-H gel might involve a reaction between the CO_2 and the Ca^{2+} ions in the interlayer zone to form a Si-rich C-S-H gel, and a silica gel. Moreover, alumina or another compound with Al tetrahedral could be formed from the Al replacing the Si in the C-S-H gel.

Acknowledgements

The authors wish to thank the MEC for the funding for project MAT2001-1490. They are likewise grateful to Prof. T. Vázquez for his valuable suggestions for this research. The authors wish to thank A. Gil and J. L. García for their collaboration in the carbonation test. M. Palacios also wishes to thank the CAM for the fellowship awarded.

REFERENCES

[1] A. M. Neville. "Properties of Concrete" Ed. Addison Wesley Longman. 4th Edition (1995)

[2] N. R. Short, A. R. Brough, A. M. G. Seneviratne, P. Purnell, C. L. Page. "Preliminary investigations of the phase composition and fine pore structure of super-critically carbonated cement pastes" J. Mat. Sci. 39 (2004) 5683-5689

[3] F. Matsushita, Y. Aono, S. Shibata. "Calcium silicate structure and carbonation shrinkage of a tobermorite-based material" Cem. Concr. Res. 34 (2004) 1251-1257

[4] F. Puertas, M. Palacios, T. Vázquez. "Carbonation process of alkali-activated slag mortars". J. Mat. Sci. 41 (2006) 3071-3082

[5] J. Deja. "Carbonation Aspects of Alkali Activated Slag Mortars and Concretes. Sil. Ind. 67 (3-4) (2002) 37-42

[6] T. Bakarev, J. G. Sanjayan, Y-B Cheng. "Resistance of alkali-activated slag concrete to carbonation" Cem. Concr. Res. 31 (2001) 1277-1283

[7] X. Bin, P. Xincheng "Study on durability of solid alkaline AAS cement" 2nd Int. Conf. Alkaline Cements and Concretes (1999) 64 - 71

[8] S. Takashima. "Systematic dissolution of calcium silicate in comercial Pórtland cement by organic acid solution". Rev. 12th General Meeting held in Tokyo. Japan Cement Engineering Association (1958) 12-13

[9] H. Moenke.- Mineralspektren. Akademie Verlag. Berlín (1962)

[10] T. Vázquez. "Contribución al estudio de las reacciones de hidratación del cemento Portland por espectroscopía infrarroja" Ph. D., Complutense University, Madrid, Spain (1975)

[11] R.J. Kirkpatrick and Xian-Dong Cong. "An introduction to ^{27}Al and ^{29}Si NMR spectroscopy of cements and concretes". Application of NMR spectroscopy to cement science. Ed. Colombet, Grimmer (1994) 55-76

[12] G. Engelhardt, D. Michel. High resolution solid-state of silicates and zeolites. Ed. John Wiley and Sons (1987)

[13] Y. Masuda, H. Tanano. "Prediction model for progress of concrete carbonation" Durability of Building Materials and Components 6, Vol. 2. Omiya (Japan) (1993). Ed. Nagataki, Nireki and Tomosowa. 1152-1161

[14] A. Fernández-Jiménez, F. Puertas, I. Sobrados and J.Sanz. "Structure of calcium silicate hidrates formed in alkaline activated slag. Influence of the type of alkaline activator". J. Am. Ceram. Soc., 86 [8] (2003) 1389-1394

[15] I. G. Richardson. "Tobermorite/jennite- and tobermorite/calcium hydroxide-based models for the structure of C-S-H: applicability to hardened pastes of tricalcium silicate, β-dicalcium silicate, Portland cement, and blends of Portland cement with blast-furnace slag, metakaolin, or silica fume" Cem. Concr. Res. 24 (2004) 1733-1777

[16].- M. Palacios. "Effect of organic admixtures in the properties of alkali-activated slag cements and mortars" PhD, Autonoma University, Madrid, Spain (2006)